Visible Transparent, UV-blocking Polymer Nanocomposite Films Containing Nano-sized Organic-LDH (Layered Double Hydroxide) Hybrid

Yan Zhao[1], Weidong Yang[2], Xungai Wang[1], Tong Lin[1]

1. Centre for Material and Fibre Innovation, Deakin University, Geelong, VIC 3217, Australia
2. Division of Materials Science & Engineering, CSIRO, Highett, VIC 3190, Australia

Abstract

A nano-sized Mg_2Al layered double hydroxide (LDH) was used for encapsulating an organic UV absorber, 2-hydroxy-4-methoxybenzeophenone-5-sulfonic acid (HMBS), to produce HMBS@LDH hybrid nano-platelets. Upon dispersing this organic-inorganic hybrid LDH into ethylene-vinyl alcohol copolymer (EVOH) for film casting, a thin polymer nanocomposite film that is UV opaque but highly transparent to visible light (higher than 90%) was formed. Thermogravimetry (TG) analysis confirmed that the intercalation of HMBS into LDH considerably increased the thermal stability of HMBS. Such an improvement was attributed to the strong guest-host interaction between the HMBS anions and the LDH layers. Also, the nanocomposite films were flexible and had good mechanical properties.

Keywords: UV-blocking; LDHs; EVOH; transparency; organic-inorganic hybrids

1. Introduction

Ultraviolet (UV) damage has been a major concern not only in daily life but also for many industries. The basic strategy of avoiding UV damage has been the use of a protective layer to shield UV light. For this purpose, a thin film or coating that contains a strong UV absorber is typically employed. Most commonly used UV absorbers are inorganic oxides, such as ZnO and TiO_2, because of the strong UV absorption and transparency in visible region. However, the main issue associated with inorganic UV absorbers is their photochemical reactivity, which can cause damage to the contacting organic material (e.g. polymer matrix) upon irradiation with UV light. Although organic UV absorbers seldom have this problem, they are typically low in thermal stability and easily migrate off the polymer matrix during use, which might lead to health problems.

Layered double hydroxides (LDHs) are inorganic layered materials consisting of stacks of positively charged hydroxide layers with hydrated charge-balancing anions between them. The chemical composition of LDH can be expressed as $[M^{2+}_{1-x}M^{3+}_{x}(OH)_2]A^{n-}_{x/n}\cdot mH_2O$, wherein M^{2+} and M^{3+} are divalent and trivalent metal ions capable of occupying the octahedral positions of the host layers and A^{n-} is the interlayer anion. The positive charges on

the hydroxide derive from the partial substitution of divalent metal ions with trivalent ones. LDHs have recently received increasing attention owing to their versatility to host a wide range of metal ions and various functional anions.[1-4] Intercalation of anionic organic molecules, such as dyes and UV absorbers, into LDH interlayer gallery has been reported, and the properties of the guest species can be modulated through guest-host interactions.[5-9] Considerably improved thermal-stability has been observed when organic UV absorbers were intercalated into LDHs. UV absorber-intercalated LDH hybrids have been reported to improve the photostability of polypropylene.[10,11] However, these materials met problem with poor transparency in visible region. For some applications, optoelectronic devices for instance, the visible transparency is vital, but still remains challenging to achieve.

In this work, we report on the preparation of visibly-transparent but UV-blocking polymer composite films by using nano-sized LDH that was intercalated with an organic UV absorber. When such hybrid nano-platelets were dispersed into ethylene-vinyl alcohol copolymer (EVOH), the resulting film did not transmit UV light, but showed high transmittance in the visible region (higher than 90%). The nanocomposite films were flexible and had good mechanical properties and high thermal stability.

2. Results and discussion

2.1. Synthesis of LDH nanocrystals

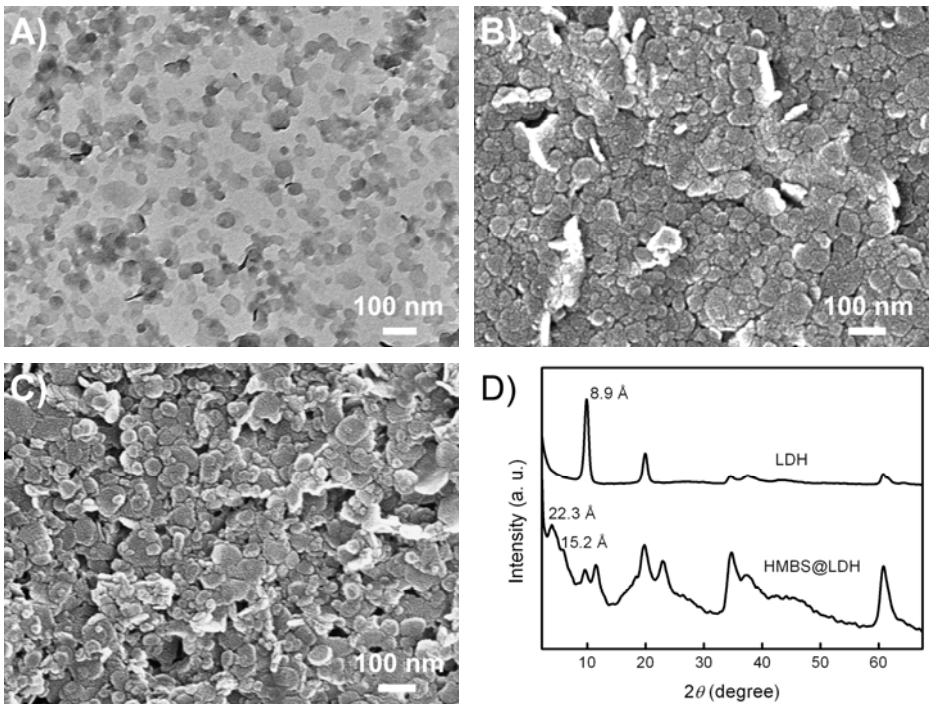

Figure 1. A) TEM and B) SEM images of the as-prepared LDH nanocrystals. C) SEM image of HMBS@LDH nanocrystals. D) XRD patterns of LDH and HMBS@LDH nanocrystals.

$Mg_2Al–NO_3$ LDH was prepared by co-precipitation of magnesium and aluminium nitrates in methanol in the presence of NaOH, followed by solvothermal treatment and hydrolysis of the methoxide ions in water.[12-14] Based on the elemental analysis and thermogravimetric measurement, the resulting LDH was formulated as $[Mg_2Al(OH)_6]NO_3 \cdot 1.5H_2O$. Figure 1A and B show the transmission electron microscopy (TEM) and scanning electron microscopy (SEM) images of the obtained LDH nanocrystals. The average lateral size of the nanocrystals was less than 100 nm.

The powder X-ray diffraction (XRD) pattern of the LDH sample is shown in Figure 1D. Several rational orders of (00*l*) reflections are observed in the diffraction pattern, indicating a hexagonal lattice with a rhombohedral symmetry. Since no other peaks were detected, the product should have high purity. The diffraction pattern and measured basal spacing (~8.96 Å) are consistent with those of well-known LDH materials intercalated with NO_3^- anions.[15] Based on the full width at half maximum (fwhm) of the (00*l*) reflection, the thickness of the LDH crystals can be estimated using Scherrer equation, being ~13.2 nm. Since the basal spacing is 8.96 Å, the thickness value of 13.2 nm suggests that the obtained crystallites contain stacks of up to 15 LDH layers.

2.2 Intercalation of HMBS into LDH nanocrystals

It is known that HMBS is a dibasic acid having both a strong sulfonic acid group ($pK_a \approx 1.6$) and a much weaker phenolic group ($pK_a \approx 8$).[16] The monovalent and divalent HMBS sodium salts exhibited very different UV-vis spectra (Figure 2). In our case, a solution containing monovalent HMBS anions was used to exchange the nitrate ions of LDHs, yielding a light-yellow product, HMBS@LDH. The UV-vis spectrum of the product indicates that the HMBS species presented in the LDH interlayers was a mixture of monovalent and divalent anions, while the UV-vis spectrum of the supernatant solution still corresponded to that of the monovalent anions (Figure 2). The presence of divalent HMBS anions in the LDH interlayers can be ascribed to the easy conversion of the monovalent to divalent anions occurred within the LDH interlayers via the reaction:[16]

$$2HMBS^-@LDH \leftrightarrow HMBS^{2-}@LDH + HMBS\ (aq)$$

The XRD pattern of the HMBS@LDH powder is shown in Figure 1D. The interlayer distance of the nanocrystals was increased from 8.9 Å to 15.0 Å and 20.2 Å, which can be assigned to the intercalation of HMBS as divalent and monovalent anions, respectively.[6] The lateral size of the HMBS@LDH crystals was comparable to the original LDH crystals (Figure 1C).

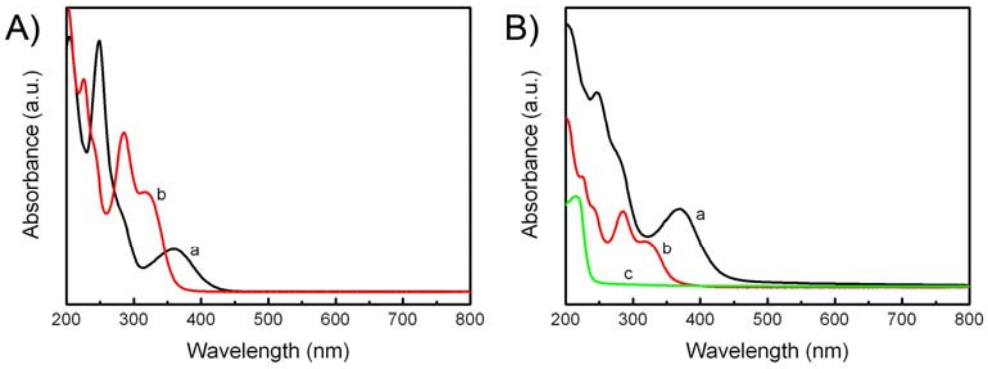

Figure 2. A) UV-vis spectra of (a) divalent and (b) monovalent HMBS sodium salts. B) UV-vis spectra of (a) HMBS@LDH nanocrystals, (b) supernatant HMBS solution after intercalation, and (c) LDH nanocrystals.

The intercalation of HMBS into LDH is also supported by the Fourier transform infrared (FTIR) spectra shown in Figure 3. For the LDH only, the intense absorption peak at 1384 cm^{-1} is attributed to N–O stretching vibrations of NO_3^- ions. HMBS is characterized by absorption bands at 1085 and 1026 cm^{-1} (sulphonate νSO_3^-); 1352 cm^{-1} (νR–SO_2–OH); 1273 cm^{-1} (νAr–O–CH_3); 1595, 1492, and 1447 cm^{-1} (aromatic ring νC=C); and 1631 cm^{-1} (carbonyl νC=O). After the intercalation of HMBS into LDHs, the characteristic absorption bands of HMBS appeared in the spectrum of HMBS@LDH, and N–O stretching vibrations of NO_3^- ions is considerably reduced, indicating the successful intercalation of HMBS anions into the interlayer galleries of the LDHs. Compared to those of free HMBS, the variation in the band positions and intensities is ascribed to the interaction between the intercalated HMBS molecules and the host LDH layers.[5]

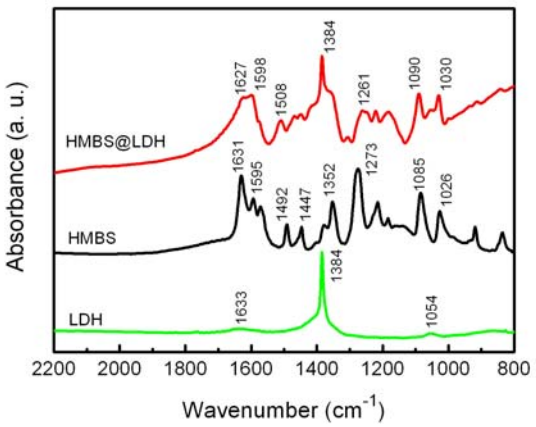

Figure 3. FTIR spectra of LDH, HMBS, and HMBS@LDH.

To examine the influence of the LDH layers on the thermal stability of the intercalated HMBS, thermogravimetric (TG) analysis was performed. The TG curves of LDH, HMBS, and HMBS@LDH are shown in Figure 4. The LDH lost weight mainly in the temperature ranges of 100−220 ºC and 300-550 ºC. The former corresponds to the removal of interlayer water molecules, while the later

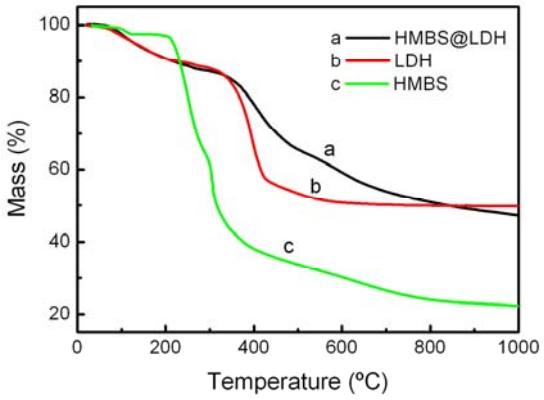

Figure 4. TGA curves of HMBS, LDH nanocrystals, and HMBS@LDH nanocrystals.

corresponds to the dehydroxylation of the brucite-like layers and the decomposition of the interlayer nitrate anions. HMBS started losing weight at about 100 ºC, which is attributed to the evaporation of the water absorbed. The main weight loss occurred between 200 and 400 ºC in two very close stages due to the decomposition of HMBS. For HMBS@LDH, the loss of the interlayer water exhibited almost the same tendency as that of LDH. At above 300 ºC, the dehydroxylation of the layers overlaps with the thermal decomposition of the intercalated HMBS. In comparison with the TG curves between the HMBS and HMBS@LDH, it was clearly indicated that the intercalated HMBS was greatly enhanced in the thermal stability.

2.3. Preparation of HMBS@LDH-EVOH nanocomposites

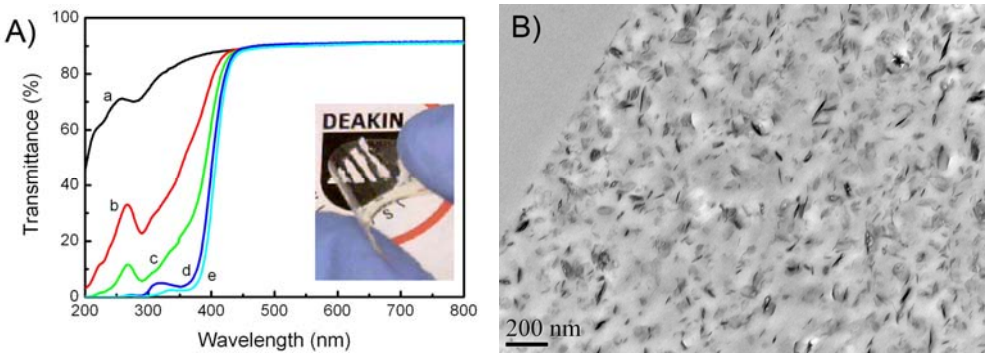

Figure 5. A) UV-vis spectra of (a) EVOH matrix and HMBS@LDH-EVOHnanocomposite films with HMBS@LDH loadings of (b) 2, (c) 5, (d) 10 and (e) 15 wt%, respectively. The inset shows a transparent and flexible film. B) TEM image of HMBS@LDH-EVOH nanocomposite film (15 wt% HMBS@LDH).

HMBS@LDH-EVOH nanocomposites were fabricated through a simple solution-mixing method. The UV-vis transmission spectra of pure EVOH and HMBS@LDH-EVOH composite films are shown in Figure 5A. The composite film exhibited significant decrease of transmittance in the UV region (< 400 nm), however its transmittance in the visible region maintained as high as 90%, which was almost the same as that of the pure EVOH film in the same region. The inset image of Figure 5A shows an optically transparent and flexible composite film with 15 wt% HMBS@LDH loading.

Figure 5B shows a typical TEM image of HMBS@LDH-EVOH nanocomposite film with 15 wt% HMBS@LDH loading. It was revealed that the HMBS@LDH crystals were homogeneously dispersed in the EVOH matrix without the formation of

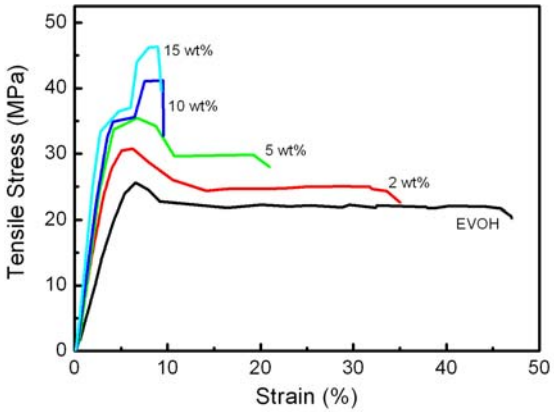

Figure 6. Stress-strain curves of pure EVOH and HMBS@LDH-EVOH nanocomposite films.

aggregates, which guarantees the good visible light transparency of the composite films.

The stress-strain curves of the pure EVOH and HMBS@LDH-EVOH composite films are revealed in Figure 6. Pure EVOH film showed a typical behavior of plastic materials with significant yielding. The addition of HMBS@LDH to EVOH led to decrease in the elongation at break of the film. The Young's modulus and tensile strength of the composite films were increased. The tensile strength increased to 30.7 and 46.5 MPa when the composite films contained 2 and 15 wt% HMBS@LDH, respectively. The enhanced mechanical properties of the composite films arose from the interaction between HMBS@LDH and the EVOH matrix. Also, the composite film was very flexible.

3. Conclusions

We have prepared a flexible polymer composite film that has an excellent ability to block UV light but highly transparent to visible light using an organic UV absorber-intercalated LDH. FTIR spectra indicate that there is a supramolecular structure with significant host-guest interaction between the host LDH layers and the guest UV absorbers. TG results show that the thermal stability of the UV absorbers was greatly increased after intercalation in LDH. The UV absorber-intercalated LDH hybrids can be incorporated into EVOH matrix to form a transparent composite film, which showed UV-blocking property, flexibility, and good mechanical property.

Experimental

Materials: Ethylene-vinyl alcohol copolymer (EVOH) with a nominal ethylene content of 44 mol%, $Mg(NO_3)_2 \cdot 6H_2O$, and $Al(NO_3)_3 \cdot 9H_2O$ were purchased from Sigma-Aldrich. UV absorber 2-hydroxy-4-methoxybenzophenone-5-sulfonic acid (HMBS) was obtained from Riedel-de Haën. Dimethyl sulfoxide (DMSO) supplied by Ajax Chemicals was of analytical grade. All chemicals were used as received.

Synthesis of LDH nanocrystals: Mg_2Al LDH (2:1 Mg/Al molar ratio) nanocrystals were prepared by a co-precipitation method. Briefly, 20 mL methanol solution containing $Mg(NO_3)_2 \cdot 6H_2O$ and $Al(NO_3)_3 \cdot 9H_2O$, in molar ratios of 2:1 was added dropwise into 80 mL NaOH (~18 mmol) solution in methanol under refluxing conditions. The mixture was then transferred into a Teflon-lined autoclave and aged at 150 ºC for 24 h. After centrifuging, the precipitate was dispersed in water to hydrolyze the methoxide with constant stirring overnight.

Synthesis of HMBS@LDH nanocrystals: HMBS was intercalated into the nitrate form LDH by mixing 30 mL of LDH suspension in water (~0.85 wt%) with 20 mL of HMBS aqueous solution (~32 mmol/L) at room temperature overnight. The pH value of the HMBS solution was adjusted to be about 7 with 1 M NaOH aqueous solution before use. The obtained solid was washed thoroughly with deionized water by centrifugation and kept in a wet state for further use.

Preparation of HMBS@LDH-EVOH nanocomposites: A desired amount of HMBS@LDH nanocrystals was dispersed into a DMSO solution containing 5 wt% EVOH under ultrasonication until the solution became transparent. The nanocomposite film was prepared by casting the solution on a glass substrate and drying in 95 ºC oven for 3 h.

Characterization techniques: Transmission electron microscopy (TEM) was performed on a JEOL JEM-2100 microscope at an acceleration voltage of 200 kV. For nanocomposite films, the samples were embedded in epoxy resin and then ultramicrotomed into 90 nm-thick sections. Scanning electron microscopy (SEM) images were taken on a ZEISS Supra 55 VP equipment operated at an acceleration voltage of 20.0 kV. Powder X-ray diffraction (XRD) data were collected on A Bruker D8 Advance X-ray Diffractometer with CuKa radiation (40kV, 40mA) monochromatised with a graphite sample monochromator over the 2-theta range of 1-71°. UV-visible spectra were recorded using a Varian Cary 3 spectrophotometer. Fourier transform infrared (FTIR) spectra were recorded on a Bruker VERTEX 70 instrument with a resolution of 4 cm^{-1} accumulating 32 scans. The specimens were prepared by using the pressed KBr disk technique. Thermogravimetric analysis (TGA) was carried out with a Netzsch STA 409 PC instrument at a heating rate of 10 ºC/min in air.

References

[1] F. Leroux, C. Taviot-Gueho, *Journal of Materials Chemistry* **2005**, *15*, 3628.
[2] A. I. Khan, D. O'Hare, *Journal of Materials Chemistry* **2002**, *12*, 3191.
[3] G. R. Williams, T. G. Dunbar, A. J. Beer, A. M. Fogg, D. O'Hare, *Journal of Materials Chemistry* **2006**, *16*, 1222.
[4] G. R. Williams, T. G. Dunbar, A. J. Beer, A. M. Fogg, D. O'Hare, *Journal of Materials Chemistry* **2006**, *16*, 1231.
[5] Y. J. Feng, D. Q. Li, Y. Wang, D. G. Evans, X. Duan, *Polymer Degradation and Stability* **2006**, *91*, 789.
[6] L. Perioli, M. Nocchetti, V. Ambrogi, L. Latterini, C. Rossi, U. Costantino, *Microporous and Mesoporous Materials* **2008**, *107*, 180.
[7] Q. He, S. Yin, T. Sato, *Journal of Physics and Chemistry of Solids* **2004**, *65*, 395.
[8] S. Mandal, D. Tichit, D. A. Lerner, N. Marcotte, *Langmuir* **2009**, *25*, 10980.
[9] X. R. Wang, J. Lu, W. Y. Shi, F. Li, M. Wei, D. G. Evans, X. Duan, *Langmuir*, *26*, 1247.
[10] D. Q. Li, Z. J. Tuo, D. G. Evans, X. Duan, *Journal of Solid State Chemistry* **2006**, *179*, 3114.
[11] G. J. Cui, X. Y. Xu, Y. J. Lin, D. G. Evans, D. Q. Li, *Industrial & Engineering Chemistry Research*, *49*, 448.
[12] E. Gardner, K. M. Huntoon, T. J. Pinnavaia, *Advanced Materials* **2001**, *13*, 1263.
[13] J. A. Gursky, S. D. Blough, C. Luna, C. Gomez, A. N. Luevano, E. A. Gardner, *Journal of the American Chemical Society* **2006**, *128*, 8376.
[14] P. Gunawan, R. Xu, *Chemistry of Materials* **2009**, *21*, 781.
[15] J. Bin Han, J. Lu, M. Wei, Z. L. Wang, X. Duan, *Chemical Communications* **2008**, 5188.
[16] K. R. Franklin, E. Lee, C. C. Nunn, *Journal of Materials Chemistry* **1995**, *5*, 565.